ISSN No:-2456-2165

Lid-Driven Square Cavity: Laminar and Turbulent Flow Visual Results on 32x32, 64x64 and 128x128 Meshgrids

Santhana Krishnan Narayanan
PG and Research Department of Computer Science,
Dr. Ambedkar Government Arts College,
Chennai, Tamilnadu, India

Antony Alphonnse Ligori
Department of Mathematics,
Gedu College of Business Studies,
Royal University of Bhutan, Bhutan

Jagan Raj Soundaraj
Department of Chemistry,
Velammal Institute of Technology,
Panjetty, Tamil Nadu, India

Abstract:- Finite volume discretization method are applied to solve the incompressible Navier-Stokes equations with primitive variables in a non-dimensional form, multigrid techniques were used to simulate the two-dimensional square driven cavity with small to large Reynolds numbers. The flow problem of constant velocity from right to left of a square cavity is considered and obtained a numerical solutions on 3 grid levels, having 32x32, 64x64 and 128X128 cells. Reynolds number of $1x10^2$, $1x10^3$ was selected for laminar flow and $8x10^3$, $12x10^3$ was selected for turbulent flow. At low and high Reynolds numbers, numerical solutions for square driven cavity flow are obtained and their results are compared to those obtained by other researchers using different approximation methods.

Keywords:- *Incompressible Navier-Stokes Equations, Finite Volume Method, Square Driven Cavity Problem, Discretization, Internal Flow.*

I. INTRODUCTION

Modeling fluid dynamics processes representing flows of an incompressible viscous fluid has been done using the Navier-Stokes equations. Direct solution approaches based on Gaussian elimination require a lot of computer memory, so iterative solutions are generally preferred. The mesh size, type of boundary conditions, and other factors improve the sustainability of classical iterative methods like Jacobi and SOR. Because of its usefulness in practical applications, iterative methods have been used to solve the incompressible Navier-Stokes equations.

The development of a phased finite-volume pressure correction method for solving incompressible Navier-Stokes equations with broad Reynolds numbers has recently piqued interest. However, the computational benefits of these compact schemes have not been thoroughly explored until recently. Because of the limitations of available computer technology and the complexity of solving the resulting Navier-Stokes equation with conventional SOR style iterative methods, it is unclear if these schemes can be used to solve incompressible Navier-Stokes equations with very large Reynolds numbers.

Developments in computer hardware with 10^{th} Generation Intel@core*i7 processor workstation computer system as well as in the analysis and attempts at various lists, such as Lid-driven square cavity, have been enabled owing to sophisticated numerical algorithms. Harlow et al. [1] developed a new method for numerical investigation of the time dependent flow of an incompressible fluid at the boundary of which is partially confined and partially free.

Ghia et al. [2] investigated the efficacy of the Coupled Highly Implicit Multi Grid (CSI-MG) method was used to test high-refine-mesh flow solutions using the vorticity-stream function formulation of the two-dimensional Navier-Stokes incompressible equations. Carbs et al. [3] solved the flow issue in a square cavity with a constant speed lid. Zhang [4] found that in fourth-order compact finite difference schemes, multi-grid techniques are used to model the two-dimensional square-driven cavity flow with small to large Reynolds numbers.

Erturk et al. [5] examined numerical calculations for 2-D steady incompressible driven cavity flow. Gupta [6] solved a driven cavity problem for $Re \leq 2000$, used the SOR iterative method with these schemes. and Zhang [7] using the fourth-order compact scheme and multigrid techniques, a high-precision solution to the conventional diffusion equation with very large Reynolds numbers was computed.

The current research is an extension to a previous study [8-9] uses a uniform surface, a finite-volume pressure correction system is combined with a 2nd order Adams-Bashforth time advancement scheme. In order to solve steady state incompressible problems, a Cartesian staggered grid is used. The square driven cavity problem exemplifies Navier-Stokes equations for large Reynolds numbers.

II. MATHEMATICAL MODEL

Although there is no analytical solution and there are singularities at two of its corners, the steady flow of an incompressible viscous fluid in a square cavity Ω=(0,1)x(0,1) has been used as a model problem by researchers for many years to test their novel numerical schemes and solution approaches.

The considered physical system has a steady state two dimensional (2-D) length L of lid-driven square cavity is represented in figure 1. The flow inside a square cavity of which the top wall (*lid y=1*) is moving with a uniform velocity from right to left and is described by the Navier-Stokes equations. Here, u and v are the parameters of the velocity vectors x and y directions, ρ and μ are the fluid density and their constant viscosity.

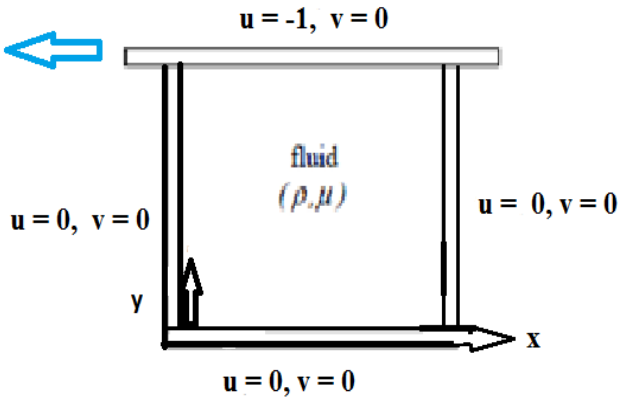

Figure 1 – Physical system of Lid-driven Square Cavity

The incompressible two dimensional Navier-Stokes equations with the lid velocity U_{Lid} , the mass and momentum equations can be written in dimensionality form as

$$\frac{\partial u'}{\partial x'} + \frac{\partial v'}{\partial y'} = 0$$

$$\rho\frac{\partial u'}{\partial t'} + \rho u'\frac{\partial u'}{\partial x'} + \rho v'\frac{\partial u'}{\partial y'} = -\frac{\partial p'}{\partial x'} + \left(\frac{\mu\partial^2 u'}{\partial x'^2} + \frac{\mu\partial^2 u'}{\partial y'^2}\right)$$

$$\rho\frac{\partial v'}{\partial t'} + \rho u'\frac{\partial v'}{\partial x'} + \rho v'\frac{\partial v'}{\partial y'} = -\frac{\partial p'}{\partial y'} + \left(\frac{\mu\partial^2 v'}{\partial x'^2} + \frac{\mu\partial^2 v'}{\partial y'^2}\right)$$

After non-dimensionalising, the mass and momentum equations can be written as

$$\frac{\partial u}{\partial x} + \frac{\partial v}{\partial y} = 0$$

$$\frac{\partial u}{\partial t} + u\frac{\partial u}{\partial x} + v\frac{\partial u}{\partial y} = -\frac{\partial p}{\partial x} + \frac{1}{Re}\left(\frac{\partial^2 u}{\partial x^2} + \frac{\partial^2 u}{\partial y^2}\right)$$

$$\frac{\partial v}{\partial t} + u\frac{\partial v}{\partial x} + v\frac{\partial v}{\partial y} = -\frac{\partial p}{\partial y} + \frac{1}{Re}\left(\frac{\partial^2 v}{\partial x^2} + \frac{\partial^2 v}{\partial y^2}\right)$$

Here $u = \frac{u'}{U_{lid}}, = \frac{v'}{U_{lid}}, x = \frac{x'}{L_{lid}}, y = \frac{y'}{L_{lid}}$,

$t = t'\frac{U_{lid}}{L_{lid}}, \rho = \frac{\rho'}{\rho_{ref}}, \mu = \frac{\mu'}{\mu_{ref}}$,

$p = \frac{p'-p_{ref}}{\rho U_{lid}^2}$ with *Re* being the Reynolds number,

$Re = \frac{\rho' U_{lid} L_{lid}}{\mu'}$ and *p* is the pressure.

No slip boundary condition has been applied for *u* and *v* directions at bottom and side walls as

$$u = 0 \; and \; v = 0$$

and in the top wall

$$u = U_{lid} = -1 \; and \; v = 0$$

Finite volume central difference discretization's can be used to express momentum equations, where *i* and *j* are cell indices on the staggered grid in the x and y directions, respectively.

$$\frac{\partial u}{\partial t} = \frac{u_{i,j}^{n+1} - u_{i,j}^{n}}{\Delta t} + O(\Delta t)$$

$$u\frac{\partial u}{\partial x} = (u_e + u_w)\frac{(u_e - u_w)}{\Delta x_u} + O(\Delta x_u^2)$$
$$= \frac{(u_e^2 - u_w^2)}{\Delta x_u} + O(\Delta x_u^2)$$

where

$$u_e = \frac{1}{2}(u_{i.j} + u_{i+1,j})$$

$$u_w = \frac{1}{2}(u_{i-1.j} + u_{i,j})$$

$$v\frac{\partial u}{\partial y} = (v_n + v_s)\frac{(u_n - u_s)}{\Delta y_v} + O(\Delta y_v^2)$$
$$= \frac{(u_n v_n - u_s v_s)}{\Delta y_v} + O(\Delta y_v^2)$$

where

$$u_n = \frac{1}{2}(u_{i.j} + u_{i,j+1})$$

$$u_s = \frac{1}{2}(u_{i.j-1} + u_{i,j})$$

$$v_n = \frac{1}{2}(v_{i-1.j+1} + v_{i,j+1})$$

$$v_s = \frac{1}{2}(v_{i-1.j} + v_{i,j})$$

$$\frac{\partial p}{\partial x} = \frac{P_{i,j} - P_{i-1,j}}{\Delta x_s} + O(\Delta x_s^2)$$

$$\frac{\partial^2 u}{\partial x^2} = \frac{\left(\frac{\partial u}{\partial x}\right)_e - \left(\frac{\partial u}{\partial x}\right)_w}{\Delta x_s} + O(\Delta x_s^2)$$

where

$$\left(\frac{\partial u}{\partial x}\right)_e = \frac{u_{i+1,j} - u_{i,j}}{\Delta x_u} + O(\Delta x_u^2)$$

$$\left(\frac{\partial u}{\partial x}\right)_w = \frac{u_{i,j} - u_{i-1,j}}{\Delta x_u} + O(\Delta x_u^2)$$

$$\frac{\partial^2 u}{\partial y^2} = \frac{\left(\frac{\partial u}{\partial y}\right)_n - \left(\frac{\partial u}{\partial y}\right)_s}{\Delta y_v} + O(\Delta x_v^2)$$

where

$$\left(\frac{\partial u}{\partial y}\right)_n = \frac{u_{i,j+1} - u_{i,j}}{\Delta y_s} + O(\Delta y_s^2)$$

$$\left(\frac{\partial u}{\partial y}\right)_s = \frac{u_{i,j} - u_{i,j-1}}{\Delta y_s} + O(\Delta y_s^2)$$

In a similar way, approximations for the y-momentum equation can be constructed. For 100≤Re≤12000, we solved the driven cavity problem. The problem was solved with several mesh sizes as to what was the coarsest mesh size that produced an acceptable solution for a given Reynolds number. Small Reynolds number solutions were largely employed to boost confidence and confirm that our method produced reliable results. For pre- and post-processing analysis, the computations were done using the MATLAB software.

III. RESULTS AND DISCUSSIONS

The upper wall of a square cavity sets the fluid inside in motion by sliding at a constant velocity from right to left. In figure 2, the viscous incompressible flow is governed by the Navier-Stokes equations and driven by the upper wall, and the domain is the unit square cavity. The Reynolds number influences viscous characteristics and pressure forces. A hierarchy of eddies develops, the large anti-clockwise rotating primary whose location occurs toward the geometric center of the square cavity and several small eddies the anti-clockwise rotating secondary eddies, the anti-clockwise rotating tertiary eddies whose locations occur at the three relevant corners of the square cavity such as bottom left, bottom right and top right are observed. All of the results in this section were obtained using uniform Cartesian grids and a finite-difference form of the Navier Stokes Equations. This results are compared with Ghia et al. [2] and found to be more accurate.

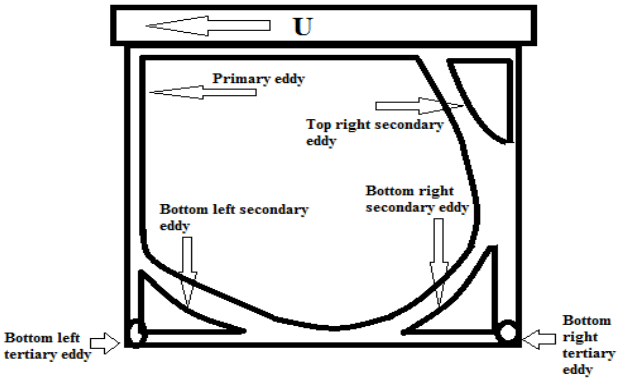

Figure 2 - Basic features of 2D flow from right to left circulation problem

The Reynolds number, *Re*, is a measure of the fluid flow's strength; as Re rises, the fluid flow becomes more energetic. This considerably facilitates research across the entire Reynolds number range, $0<Re<\infty$. Almost every phenomenon that may occur in incompressible flows may be seen in lid-driven square cavity flows, such as primary eddies, cornor eddies, corner singularities, secondary & tertiary flows. The velocity of the top boundary is set to be $u= -1.0$ and $v=0$ for all three mesh grids of *32x32, 64x64 and 128x128*.

2.1 Mesh Grid 32 x 32

As the wall velocity increases, the lid-driven square cavity flow relates to the two-dimensional flow evolution. In the absence of instability, the steady, two-dimensional flow should develop into a vortex with a viscid center of uniform vorticity surrounded by viscous boundary layers that connect the vortex center to the boundary conditions for large Reynolds numbers. However, At large Reynolds numbers, the two-dimensional steady flow is not stable and smaller scale vortices are shed from the downstream end of the moving wall into the cavity when the Reynolds number rises above a critical value.

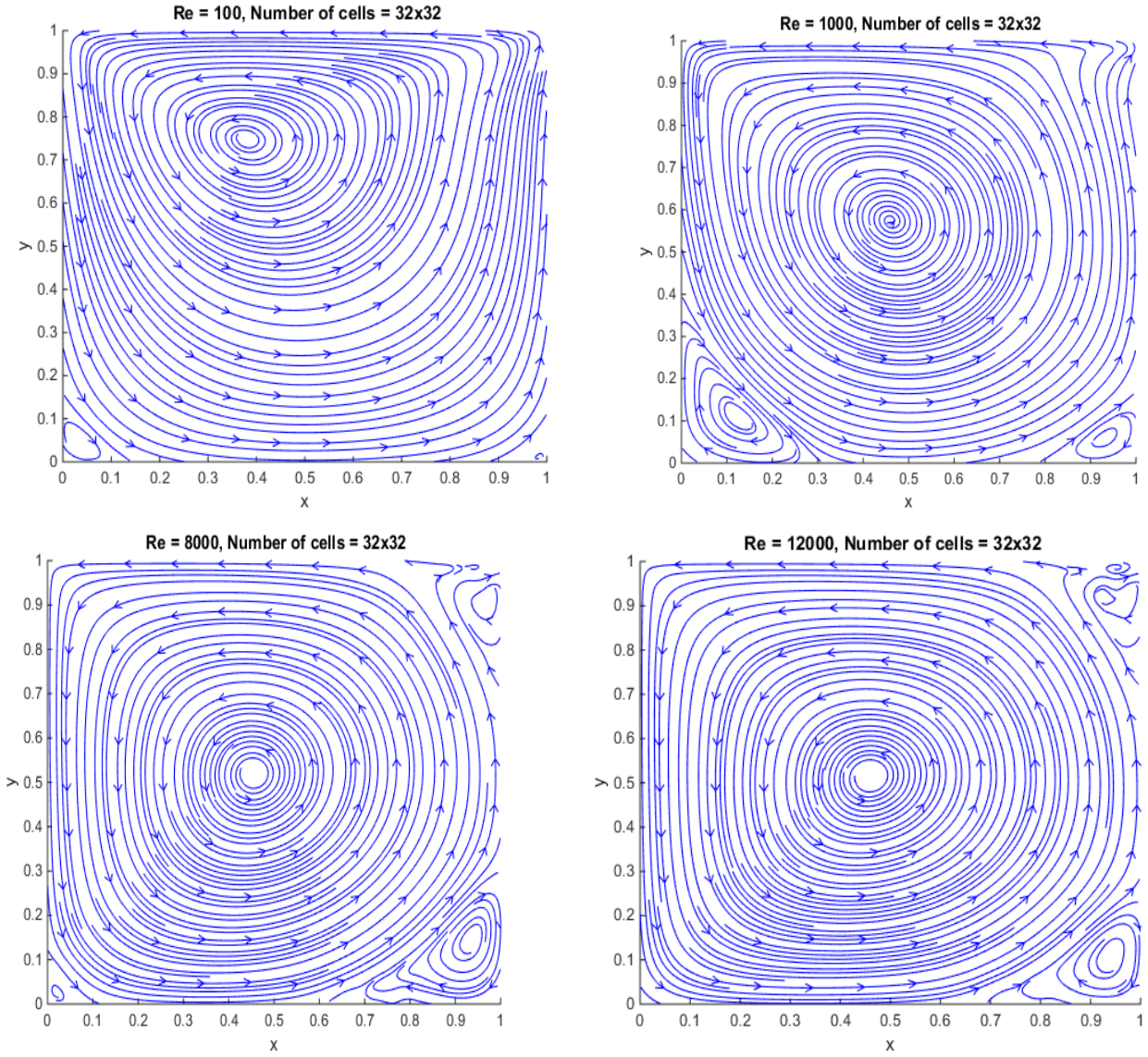

Figure 3 – Streamlines showing solution for *Laminar and Turbulent flow* on *32 x 32* grid

The visual results of Figure 3 displays standard streamline patterns of the two-dimensional global re-circulating vortex powered by the moving wall with a *32x32* grid for *Re=100, 1000, 8000 and 12000.*

- For *Re=100*, the visual results of figure 3 show streamline contours of the primary vortex accompanied by initial formation of bottom right corner secondary vortex and subsequent formation of bottom left corner secondary vortex. The center of the primary vortex is offset towards the top left corner at (0.3600, 0.7300) and moves through very slowly towards the geometric center of the cavity at (0.5000, 0.5000).
- For *Re=1000*, the visual results of figure 3 show streamline contours of the primary vortex accompanied by bottom left corner secondary vortex grows rapidly in size and subsequent development of bottom right corner secondary vortex. The center of the primary vortex is offset towards the top left corner at (0.4750, 0.5830) and moves through very slowly towards the geometric center of the cavity at (0.5000, 0.5000).
- For the broad *Re=8000*, the visual results of figure 3 show the streamline contours of the primary vortex accompanied by initial formation and subsequent growth of secondary vortex on the top right corner side of the cavity is clearly illustrated. Also, a well-developed secondary vortex formation at the bottom right corner and a subsequent formation of bottom left corner secondary vortex grows rapidly in size are identified with visual results. The center of the primary vortex is offset towards the middle at (0.4700, 0.5100) and adjust themselves slowly towards the geometric center of the cavity at (0.5000, 0.5000).
- For the broad *Re=12000*, the visual results of figure 3 show the streamline contours of the primary vortex accompanied by the formation and subsequent growth of secondary vortex on the top right corner, bottom right corner and bottom left corner of the cavity is clearly illustrated with visuals. The center of the primary vortex is offset towards the geometric center of the cavity at (0.5000, 0.5000).The results presented here comply with [2] reported solutions for fine grids.

2.2 Mesh Grid 64 x 64

Typical visual results of streamline contours of the globally recirculating two-dimensional vortex powered by the moving wall for Re=100, 1000, 8000 and 12000 with 64x64 grid are shown in figure 4.

For *Re=100*, the visual results of figure 4 show streamline contours of the primary vortex accompanied by initial formation of bottom right corner secondary vortex and subsequent formation of bottom left corner secondary vortex grows rapidly in size . The center of the primary vortex is offset towards the top left corner at (0.3650, 0.7350) and moves through very slowly towards the geometric center of the cavity at (0.5000, 0.5000).

For *Re=1000*, the visual results of figure 4 show streamline contours of the primary vortex accompanied by well-developed bottom left corner secondary vortex and subsequent development of bottom right corner secondary vortex grows rapidly in size. The center of the primary vortex is offset towards the middle at (0.5150, 0.5630) and moves through very slowly towards the geometric center of the cavity at (0.5000, 0.5000).

For the broad *Re=8000*, the visual results of figure 4 show the streamline contours of the primary vortex accompanied by initial formation and subsequent growth of secondary vortex on the top right corner side of the cavity is clearly illustrated. Also, a well-developed secondary vortex formation at the bottom right corner and a subsequent formation of bottom left corner secondary vortex grows rapidly in size are identified with visual results. Also, a tertiary vortex grows rapidly in size on the bottom left corner. The center of the primary vortex is offset towards the geometric center of the cavity at (0.5000, 0.5000).

For the broad *Re=12000*, the visual results of figure 4 show the streamline contours of the smooth primary vortex accompanied by the formation and subsequent growth of secondary vortex on the top right corner, bottom right corner and bottom left corner of the cavity is clearly illustrated with visuals. Also, the visual result indicate that there are additional tertiary vortex grows rapidly in size at bottom left corner and bottom right corner of the cavity. The center of the primary vortex is offset towards the geometric center of the cavity at (0.5000, 0.5000).The results presented here comply with [2] reported solutions for fine grids.

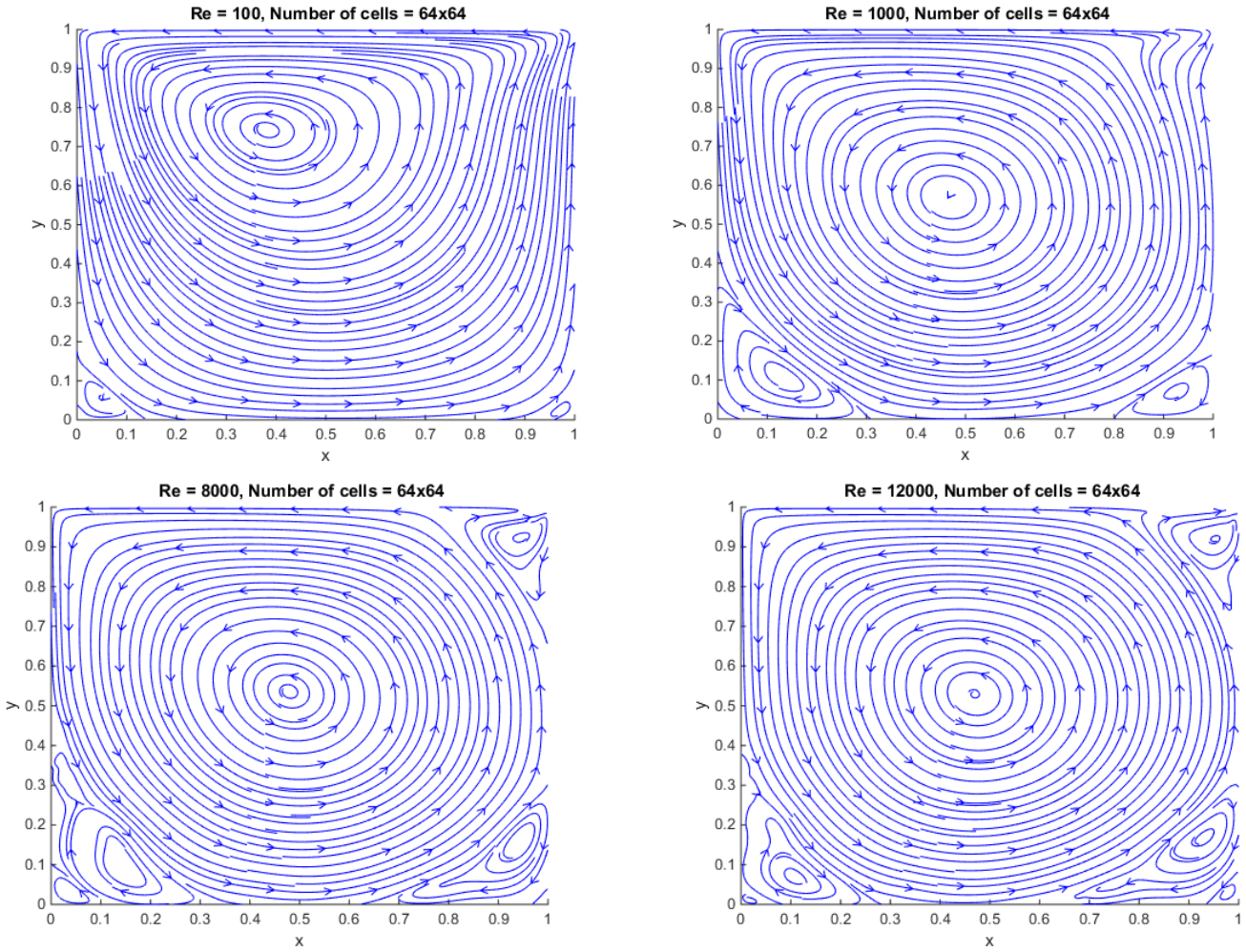

Figure 4 – Streamlines showing solution for *Laminar and Turbulent flow* on 64 *x 64* grid

2.3 Mesh Grid 128 x 128

Typical visual results of streamline contours of the globally recirculating two-dimensional vortex powered by the moving wall for Re=100, 1000, 8000 and 12000 with 128x128 grid are shown in figure 5.

- For *Re=100*, the visual results of figure 5 show streamline contours of the primary vortex accompanied by initial formation of bottom right corner secondary vortex and subsequent formation of bottom left corner secondary vortex grows rapidly in size . The center of the primary vortex is offset towards the top left corner at (0.4650, 0.7850) and moves through very slowly towards the geometric center of the cavity at (0.5000, 0.5000).
- For *Re=1000*, the visual results of figure 5 show streamline contours of the primary vortex accompanied by well-developed bottom left corner secondary vortex and subsequent development of bottom right corner secondary vortex grows rapidly in size. The center of the primary vortex is offset towards the middle at (0.5010, 0.5330) and moves through very slowly towards the geometric center of the cavity at (0.5000, 0.5000).
- For the broad *Re=8000*, the visual results of figure 5 show the streamline contours of the primary vortex accompanied by initial formation and subsequent growth of secondary vortex on the top right corner side of the cavity is clearly illustrated. Also, a well-developed secondary vortex formation at the bottom right corner and a subsequent formation of bottom left corner secondary vortex grows rapidly in size are identified with visual results. Also, a tertiary vortex grows rapidly in size on the bottom left corner. The center of the primary vortex is offset towards the geometric center of the cavity at (0.5000, 0.5000).
- For the broad *Re=12000*, the visual results of figure 5 show the streamline contours of the smooth primary vortex accompanied by the formation and subsequent growth of secondary vortex on the top right corner, bottom right corner and bottom left corner of the cavity is clearly illustrated with visuals. Also, the visual result indicate that there are additional tertiary vortex grows rapidly in size at bottom left corner and bottom right corner of the cavity. The center of the primary vortex is offset towards the geometric center of the cavity at (0.5000, 0.5000).The results presented here comply with [2] reported solutions for fine grids.

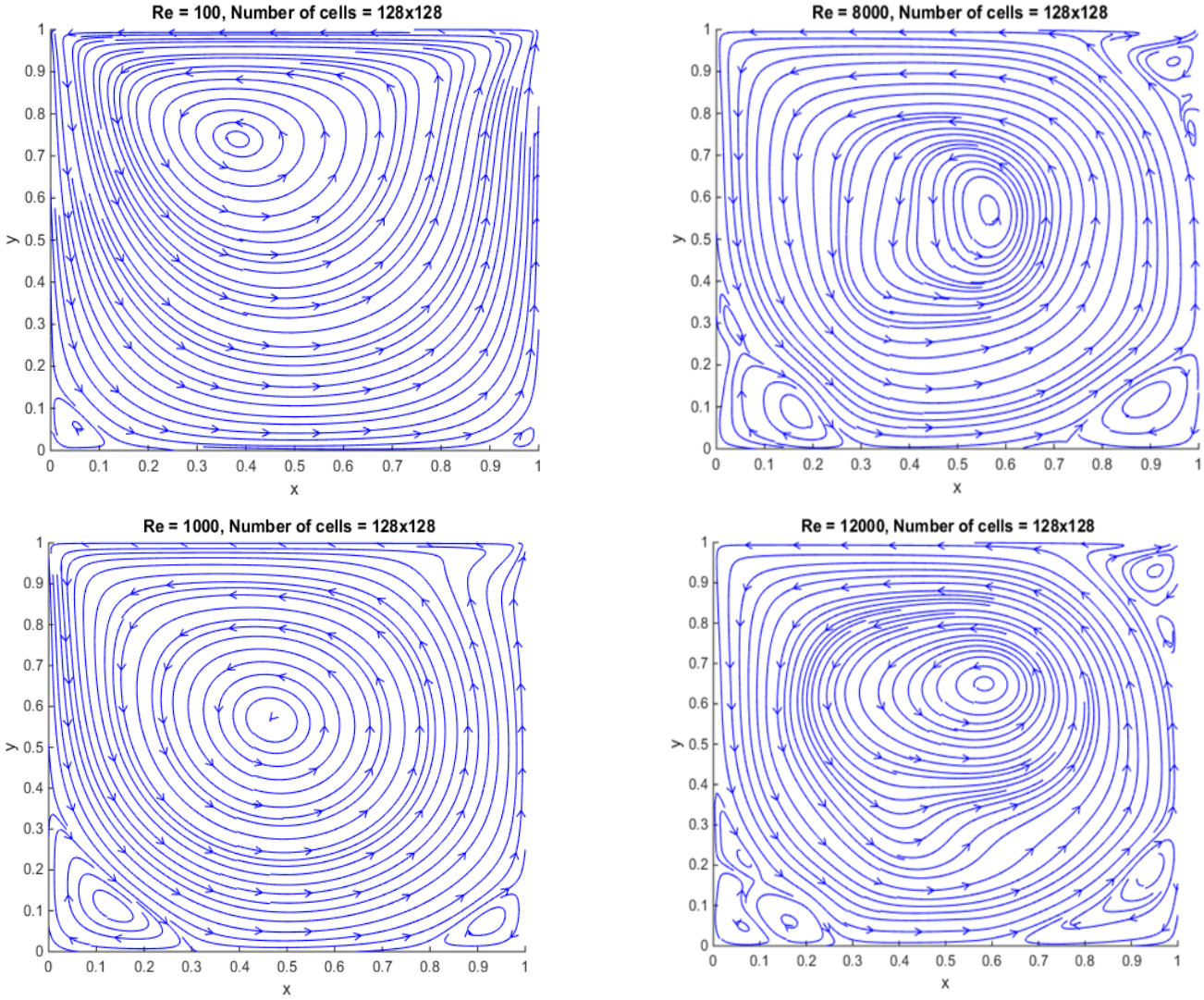

Figure 5 – Streamlines showing solution for Laminar and Turbulent flow on 128 x 128 grid

ISSN No:-2456-2165

IV. CONCLUSION

For the laminar flow with *Re=100, 1000* and turbulent flow with *Re=8000, 12000* fine mesh solutions were obtained very efficiently. The finest mesh size used in the grid series, 32x32 64x64 and 128x128, remains a very important parameter. It was shown that the smoothing factor of the iteration schemes was affected by the Reynolds number physical problem parameters. Using this Lid-driven square cavity issue, the robustness and efficiency of the overall solution techniques has been demonstrated, comprehensive specific outcomes have been presented. The present findings comply with published fine-grid solutions.

ACKNOWLEDGEMENTS

The authors thank the anonymous reviewers for their valuable comments.

REFERENCES

[1]. Harlow F.H and Welch J.E, "Numerical Calculation of Time-Dependent viscous incompressible flow of fluid with free surface", The Physics of Fluids, Vol. 3, pp. 2182-2189, 1965.

[2]. Ghia V, Ghia K and Shin C, "*High resolutions for incompressible flow using the Navier-Stokes equations and a multigrid method*", Journal of computational Physics, Vol. 48, No. 3, pp. 387-411, 1982.

[3]. Carbs H.M, Roberta S and Araki L.K, "*The Lid-driven square cavity flow : Numerical solution with a 1024x1024 grid*", Journal of the Brazil Soc. of Mech. Sci. &Engg., Vol. XXXI, No. 3/191, pp. 186-198, 2009.

[4]. Zhang J, "*Numerical simulation of 2D square driven cavity using fourth-order compact finite difference schemes*, Computers and Mathematics with Applications, Vol. 45, pp. 43-52, 2003.

[5]. Erturk E, Carke T.C and Gokcol, "*Numerical solutions of steady incompressible driven cavity flow at high Reynolds number*", International Journal of Numerical methods in Fluids, Vol. 48, pp. 747-774, 2005.

[6]. Gupta M.M, "*High accuracy solutions of incompressible Navier-Stokes equations*", J.Comut. Phys, Vol. 93, pp. 343-359, 1991.

[7]. Zhang J, "*Accelerated multigrid high accuracy solution of the convection-diffusion equation with high Reynolds number*", Numer. Methods Partial Differential Equations, Vol.13, pp. 77-92, 1997.

[8]. Santhana Krishnan Narayanan; Antony Alphonnse Ligori, Jagan Raj Soundaraj, "*Visualization Analysis of Numerical Solution With 32x32 and 64x64 Mesh Grid Lid-Driven Square Cavity Flow*", Vol. 5 Issue. 9, International Journal of Innovative Science and Research Technology (IJISRT), www.ijisrt.com. ISSN - 2456-2165, pp. 652-656, 2020.

[9]. Santhana Krishnan Narayanan; Antony Alphonnse Ligori, Jagan Raj Soundarraj. "*Stream Function-Vorticity flow in Lid-Driven Square Cavity: Computational and Visualization Analysis with Fine Mesh Grid*.", Vol. 5 Issue. 12, International Journal of Innovative Science and Research Technology (IJISRT), www.ijisrt.com. ISSN - 2456-2165, pp. 318-330, 2020.